bioRxiv preprint doi: https://doi.org/10.1101/2020.09.29.319731; this version posted September 30, 2020. The copyright holder for this preprint (which was not certified by peer review) is the author/funder. All rights reserved. No reuse allowed without permission.

1 **Inhibition of SARS-CoV-2 in Vero cell cultures by peptide-conjugated morpholino-**
2 **oligomers.**

3 Kyle Rosenke[1], Shanna Leventhal[1], Hong M. Moulton[2], Susan Hatlevig[2], David Hawman[1],
4 Heinz Feldmann[1], David A. Stein[2]*

5 [1]Laboratory of Virology, Division of Intramural Research, National Institute of Allergy and
6 Infectious Diseases, National Institutes of Health, Hamilton, MT.
7
8 [2]Department of Biomedical Sciences, Carlson College of Veterinary Medicine, Oregon State
9 University, Corvallis, OR.
10
11 *Corresponding author
12 phone: 541-231-1332
13 fax: 541-737-2730
14 email: dave.stein@oregonstate.edu
15
16

17 **Running title:** Inhibition of SARS-CoV-2 by PPMO

18

19

20

21

bioRxiv preprint doi: https://doi.org/10.1101/2020.09.29.319731; this version posted September 30, 2020. The copyright holder for this preprint (which was not certified by peer review) is the author/funder. All rights reserved. No reuse allowed without permission.

22

23 **Synopsis:**

24 **Background:** SARS-CoV-2 is the causative agent of COVID-19 and a pathogen of immense
25 global public health importance. Development of innovative direct-acting antiviral agents is
26 sorely needed to address this virus. Peptide-conjugated morpholino oligomers (PPMO) are
27 antisense agents composed of a phosphordiamidate morpholino oligomer covalently conjugated
28 to a cell-penetrating peptide. PPMO require no delivery assistance to enter cells and are able to
29 reduce expression of targeted RNA through sequence-specific steric blocking.

30 **Objectives and Methods:** Five PPMO designed against sequences of genomic RNA in the
31 SARS-CoV-2 5'-untranslated region and a negative control PPMO of random sequence were
32 synthesized. Each PPMO was evaluated for its effect on the viability of uninfected cells and its
33 inhibitory effect on the replication of SARS-CoV-2 in Vero-E6 cell cultures. Cell viability was
34 evaluated with an ATP-based method and viral growth was measured with quantitative RT-PCR
35 and $TCID_{50}$ infectivity assays.

36 **Results:** PPMO designed to base-pair with sequence in the 5'-terminal region or the leader
37 transcription regulatory sequence-region of SARS-CoV-2 genomic RNA were highly
38 efficacious, reducing viral titers by up to 4-6 log10 in cell cultures at 48-72 hours post-infection,
39 in a non-toxic and dose-responsive manner.

40 **Conclusion:** The data indicate that PPMO have the ability to potently and specifically suppress
41 SARS-CoV-2 growth and are promising candidates for further pre-clinical development.

42

bioRxiv preprint doi: https://doi.org/10.1101/2020.09.29.319731; this version posted September 30, 2020. The copyright holder for this preprint (which was not certified by peer review) is the author/funder. All rights reserved. No reuse allowed without permission.

43 **Introduction:**

44 There is a pressing need for the development of additional antiviral therapeutics to address
45 SARS-CoV-2 infections. Peptide-conjugated phosphorodiamidate morpholino oligomers
46 (PPMO) are single-stranded-nucleic acid analogs capable of entering cells without assistance and
47 interfering with gene expression through steric blockade of targeted RNA. PPMO are composed
48 of a phosphorodiamidate morpholino oligomer (PMO) covalently conjugated to a cell-
49 penetrating peptide (CPP)[1-3]. PPMO are water-soluble, nuclease resistant and non-toxic at
50 effective concentrations across a range of *in vitro* and *in vivo* applications [1, 4]. In several *in*
51 *vivo* models of respiratory viruses, including influenza A virus[5, 6], respiratory syncytial virus
52 [7]and porcine reproductive and respiratory syndrome virus[8], intranasally administered PPMO
53 targeted against virus sequence have reduced viral titer and pathology in lung tissue.

54 The 5'UTR of the coronavirus genome contains sequences and structures known to be important
55 in various aspects of the virus life-cycle including translation and RNA synthesis [9]. In previous
56 studies, PPMO targeted to various sites in the 5'UTR of mouse hepatitis virus (MHV) [10, 11]
57 and SARS-CoV [12] were effectively antiviral. In the present study we investigated the ability of
58 five PPMO targeted against various sites in the 5'UTR and polyprotein 1a/b translation start site
59 (AUG) region of SARS-CoV-2 to suppress virus growth in cell cultures. We found that PPMO
60 targeting the 5'terminal region and the transcription regulatory sequence (TRS)-leader region of
61 genomic RNA were potent inhibitors of SARS-CoV-2 replication.

62 **Materials and Methods:**

63 **Biosafety.** Work with infectious SARS-CoV-2 was approved by the Institutional Biosafety
64 Committee (IBC) and performed in high biocontainment at Rocky Mountain Laboratories

bioRxiv preprint doi: https://doi.org/10.1101/2020.09.29.319731; this version posted September 30, 2020. The copyright holder for this preprint (which was not certified by peer review) is the author/funder. All rights reserved. No reuse allowed without permission.

65 (RML), NIAID, NIH. Sample removal from high biocontainment followed IBC-approved
66 Standard Operating Protocols.

67 **PPMO synthesis.** PPMO were synthesized by covalently conjugating the CPP $(RXR)_4$ (where R
68 is arginine and X is 6-aminohexanoic acid) to PMO (Gene Tools LLC, Philomath, Oregon) at
69 the 3' end through a noncleavable linker, by methods described previously [3].

70 **Cells and viruses.** Vero-E6 cells (ATCC) were maintained in DMEM supplemented with 10%
71 fetal calf serum, 1 mM L-glutamine, 50 U/mL penicillin and 50 µg/mL streptomycin (growth
72 medium). All cell culture incubations were carried out at 37° C and 5% CO_2. SARS-CoV-2
73 isolate nCoV-WA1-2020 was kindly provided by the Centers for Disease Control and Prevention
74 (Atlanta, Georgia, USA). Preparation and quantification of the virus followed methods
75 previously described[13]. Briefly, the original virus stock was propagated once at RML in Vero-
76 E6 cells in DMEM supplemented with 2% fetal bovine serum containing L-glutamine and
77 antibiotics as above (infection medium). The virus stock used in the experiments was passage 4
78 and was confirmed by sequencing to be identical to the initial deposited GenBank sequence
79 MN985325.

80 **Cell viability assay.** Cell viability was assessed using CellTiterGlo (Promega). Vero E6 cells
81 grown in 96-well plates were incubated in the presence of PPMO in growth media for 48 hours,
82 then assayed according to the manufacturer's instructions. Statistical analysis was carried out
83 using GraphPad Prizm (San Diego, CA).

84 **Antiviral assays.** PPMO were resuspended in sterile PBS. Vero-E6 cells were plated in 48 well
85 plates and were approximately 80% confluent on the day of infection. At 5 hrs before infection,
86 the growth medium was removed and replaced with infection medium containing PPMO. For

bioRxiv preprint doi: https://doi.org/10.1101/2020.09.29.319731; this version posted September 30, 2020. The copyright holder for this preprint (which was not certified by peer review) is the author/funder. All rights reserved. No reuse allowed without permission.

87 viral infections, the PPMO-containing medium was aspirated and the cells rinsed twice with
88 DMEM before adding 100 µl of infection medium containing virus at a MOI of .01. Following a
89 one hour infection period, the virus-containing inoculum was aspirated and the cells washed
90 twice with infection medium after which 300 µl fresh infection medium was added. At 12, 24, 48
91 and 72 hours post-infection (pi), all of the media in a well was collected for qRT-PCR and
92 $TCID_{50}$ analysis.

93 **Evaluation of virus quantity by qRT-PCR.** Supernatants were harvested as described above
94 and viral RNA purified and quantified by using one-step quantitative reverse transcription PCR
95 (qRT-PCR) following previous described methods [13]. Briefly, total RNA was isolated with the
96 RNeasy Mini kit (Qiagen) and RT-PCR carried out using the One-Step RT-PCR kit (Qiagen)
97 according to the manufacturer's protocols. Copy numbers were calculated using standards
98 produced as previously described [13].

99 **$TCID_{50}$ evaluations.** Viral supernatants were serially diluted in DMEM and each dilution
100 sample was titrated in triplicate. Subsequently, 100 ul of each virus dilution was transferred to
101 Vero-E6 cells grown in 96-well plates containing 100ul DMEM. Following a seven day
102 incubation period, wells were scored for cytopathic effect (CPE). The $TCID_{50}$ values were
103 calculated via the Reed-Muench formula.

104

105 **Results:**

106 **PPMO design**. PPMO design was guided by previous studies in which various Nidoviruses were
107 targeted with PPMO [10-12, 14, 15]. In this study, five PPMO were designed to target the 5' UTR
108 and first translation start site-region of SARS-CoV-2 positive sense genomic RNA (**Table 1**). Two

bioRxiv preprint doi: https://doi.org/10.1101/2020.09.29.319731; this version posted September 30, 2020. The copyright holder for this preprint (which was not certified by peer review) is the author/funder. All rights reserved. No reuse allowed without permission.

109 of the PPMO target the 5'-terminal-region of the genome. Both 5'END-1 and 5'END-2 were
110 designed with the intention of interfering with pre-initiation of translation of genomic and
111 subgenomic mRNAs.

112 Two PPMO were designed to target the genomic 5'UTR region containing the putative SARS-
113 CoV-2 leader-TRS core sequence (nt 70-75, 5'-ACGAAC-3') and thereby potentially interfere
114 with body-TRS to leader-TRS base-pairing, and/or with translocation of the 48S translation
115 preinitiation complex along the 5'UTR of the genomic and various subgenomic mRNAs.
116 Coronaviruses produce a set of nested mRNAs through the process of discontinuous subgenomic
117 mRNA synthesis. The TRS is a six-ten nt sequence that is critical in the production of negative
118 strand mRNA templates during this process [16, 17]. For SARS-CoV, the leader-TRS core
119 sequence consists of nt 67-72 of the genomic RNA sequence[18], and most viral mRNAs possess
120 the same 72 nt 5' leader sequence.

121 The AUG PPMO was designed to target the translation initiation region for ORF1a/b, which codes
122 for the replicase polyprotein, with the intention to block translation initiation.

123 A negative control PPMO (NC) of random sequence was included (see Table 1), to control for
124 nonspecific effects of the PPMO chemistry. NC was screened using BLAST and contains little
125 significant homology to any primate, rodent or viral sequences.

126 **Evaluation of PPMO cytotoxicity.** To evaluate the effect of PPMO treatments on cell viability,
127 cells were treated under similar conditions to the antiviral assays described below, but in the
128 absence of virus. Cells were treated in triplicate with increasing doses of PPMO for 48 hours before
129 being assayed using a quantitative cell viability assay. At the concentrations used in the antiviral
130 assays described below, none of the PPMO produced more than 5% cytotoxic effect (**Figure 1A**).

bioRxiv preprint doi: https://doi.org/10.1101/2020.09.29.319731; this version posted September 30, 2020. The copyright holder for this preprint (which was not certified by peer review) is the author/funder. All rights reserved. No reuse allowed without permission.

131 **Evaluation of PPMO antiviral activity.** To determine the inhibitory activity of the various
132 PPMO on SARS-CoV-2 replication, Vero-E6 cells were treated with each of the six PPMO
133 described in Table 1 at 4, 8, and 16 μM for 5 hours before infection, then incubated without
134 PPMO after infection. Cell supernatants were collected at four time-points post-infection: 12, 24,
135 48, and 72 hours. Virus growth was evaluated by two methods, qRT-PCR and $TCID_{50}$ infectivity
136 assay. Using an MOI of 0.01, virus growth rose steadily and reached peak growth at 72 hrs post-
137 infection (**Fig. 1B and H**). Growth of the virus under PBS treatment was highly similar to virus
138 growth under NC PPMO treatment (data not shown). Four of the five PPMO designed to target
139 SARS-CoV-2 RNA were highly effective, suppressing viral titers by 3-5 log10 at the 48 and 72
140 hr time-points (**Figure 1B-M**). qPCR analysis showed that in cells treated with 8 or 16 μM of
141 any of the four PPMO targeting the 5'end- or TRS-regions, virus growth was markedly
142 suppressed at 12-48 hrs post-infection. The number of cycles required to detect virus from those
143 samples was approximately the same as the number of cycles required to detect the input virus
144 shortly after infection. At 72 hrs post-infection, the efficacy of the 5'END- and TRS-PPMO had
145 waned, to a minor extent, although still providing multi-log suppression of virus growth. The
146 AUG PPMO was not nearly as effective as the other 4 antiviral PPMO used in this study (**Figure
147 1C and I**).

148 **Discussion:**

149 We found that PPMO targeting the 5'terminal-region or leader-TRS-region were highly effective
150 at inhibiting the growth of SARS-CoV-2, whereas a PPMO targeting the polyprotein 1a/b AUG
151 translation start site region was not effective. It is unknown if the ineffective AUG-PPMO was
152 unable to bind to its target, or if duplexing occurred yet was relatively inconsequential.

bioRxiv preprint doi: https://doi.org/10.1101/2020.09.29.319731; this version posted September 30, 2020. The copyright holder for this preprint (which was not certified by peer review) is the author/funder. All rights reserved. No reuse allowed without permission.

153 To date, little sequence variation in the PPMO target sites in the 5'UTR of SARS-CoV-2 has
154 been identified. Of the whole-genome nucleotide sequences reported in GenBank, two genotypes
155 contain a single mismatch with the 5'END PPMO and one genome has a single mismatch with
156 the TRS PPMO[19]. Previous studies have shown that PPMO having a single base mismatch
157 with their target site retain approximately 90% of their activity compared to those having perfect
158 agreement [15, 20].

159 This study demonstrates that PPMO targeted against SARS-CoV-2 can enter cells readily and
160 inhibit viral replication in a sequence-specific, dose-responsive and non-toxic manner.
161 Considering the considerable *in vivo* antiviral efficacy demonstrated by PPMO against several
162 respiratory viruses in previous studies [5-8], further development of the 5'END- and TRS-PPMO
163 appears warranted.

164 **Funding:** This work was funded by the Intramural Research Program of the National Institutes
165 of Allergy and Infectious Diseases (NIAID), National Institutes of Health (NIH).

166 **Transparency declaration:** The authors have no conflicts of interest.

167

168 **References:**

169 1. Moulton, H.M. and J.D. Moulton, *Morpholinos and their peptide conjugates: therapeutic*
170 *promise and challenge for Duchenne muscular dystrophy.* Biochim Biophys Acta, 2010.
171 **1798**(12): p. 2296-303.
172 2. Moulton, H.M., and J.D. Moulton, *Antisense Morpholino Oligomers and Their Peptide*
173 *Conjugates*, in *Therapeutic Oligonucleotides*, J. Kurreck, Editor. 2008, Royal Society of
174 Chemistry: London, England. p. 43-79.
175 3. Abes, S., et al., *Vectorization of morpholino oligomers by the (R-Ahx-R)(4) peptide*
176 *allows efficient splicing correction in the absence of endosomolytic agents.* J Control
177 Release, 2006. **116**(3): p. 304-13.

bioRxiv preprint doi: https://doi.org/10.1101/2020.09.29.319731; this version posted September 30, 2020. The copyright holder for this preprint (which was not certified by peer review) is the author/funder. All rights reserved. No reuse allowed without permission.

178 4. Stein, D.A., *Inhibition of RNA virus infections with peptide-conjugated morpholino*
179 *oligomers.* Curr Pharm Des, 2008. **14**(25): p. 2619-34.
180 5. Gabriel, G., et al., *Morpholino oligomers targeting the PB1 and NP genes enhance the*
181 *survival of mice infected with highly pathogenic influenza A H7N7 virus.* J Gen Virol,
182 2008. **89**(Pt 4): p. 939-48.
183 6. Lupfer, C., et al., *Inhibition of influenza A H3N8 virus infections in mice by morpholino*
184 *oligomers.* Archives of virology, 2008. **153**(5): p. 929-37.
185 7. Lai, S.H., et al., *Inhibition of respiratory syncytial virus infections with morpholino*
186 *oligomers in cell cultures and in mice.* Mol Ther, 2008. **16**(6): p. 1120-8.
187 8. Opriessnig, T., et al., *Inhibition of porcine reproductive and respiratory syndrome virus*
188 *infection in piglets by a peptide-conjugated morpholino oligomer.* Antiviral Res, 2011.
189 **91**(1): p. 36-42.
190 9. Masters, P.S., and S. Perlman, *Coronaviridae*, in *Fields virology*, D.M. Knipe, and P.M.
191 Howley, Editor. 2013, Lippincott Williams & Wilkins: Philadelphia, PA. p. 825-858.
192 10. Burrer, R., et al., *Antiviral effects of antisense morpholino oligomers in murine*
193 *coronavirus infection models.* J Virol, 2007. **81**(11): p. 5637-48.
194 11. Neuman, B.W., et al., *Antisense morpholino-oligomers directed against the 5' end of the*
195 *genome inhibit coronavirus proliferation and growth.* J Virol, 2004. **78**(11): p. 5891-9.
196 12. Neuman, B.W., et al., *Inhibition, escape, and attenuated growth of severe acute*
197 *respiratory syndrome coronavirus treated with antisense morpholino oligomers.* J Virol,
198 2005. **79**(15): p. 9665-76.
199 13. Munster, V.J., et al., *Respiratory disease in rhesus macaques inoculated with SARS-CoV-*
200 *2.* Nature, 2020.
201 14. van den Born, E., et al., *Antiviral activity of morpholino oligomers designed to block*
202 *various aspects of Equine arteritis virus amplification in cell culture.* J Gen Virol, 2005.
203 **86**(Pt 11): p. 3081-90.
204 15. Zhang, Y.J., et al., *Suppression of porcine reproductive and respiratory syndrome virus*
205 *replication by morpholino antisense oligomers.* Vet Microbiol, 2006. **117**(2-4): p. 117-
206 29.
207 16. Sawicki, S.G., D.L. Sawicki, and S.G. Siddell, *A contemporary view of coronavirus*
208 *transcription.* J Virol, 2007. **81**(1): p. 20-9.
209 17. Pasternak, A.O., W.J. Spaan, and E.J. Snijder, *Nidovirus transcription: how to make*
210 *sense...?* J Gen Virol, 2006. **87**(Pt 6): p. 1403-21.
211 18. Yang, D. and J.L. Leibowitz, *The structure and functions of coronavirus genomic 3' and*
212 *5' ends.* Virus Res, 2015. **206**: p. 120-33.
213 19. Khailany, R.A., M. Safdar, and M. Ozaslan, *Genomic characterization of a novel SARS-*
214 *CoV-2.* Gene Rep, 2020: p. 100682.
215 20. Ge, Q., et al., *Inhibition of multiple subtypes of influenza a virus in cell cultures with*
216 *morpholino oligomers.* Antimicrob Agents Chemother, 2006. **50**(11): p. 3724-33.
217
218
219
220
221

bioRxiv preprint doi: https://doi.org/10.1101/2020.09.29.319731; this version posted September 30, 2020. The copyright holder for this preprint (which was not certified by peer review) is the author/funder. All rights reserved. No reuse allowed without permission.

222 **Table 1. Names, sequences, and target locations of SARS-CoV-2 PPMO**

PPMO name	PPMO sequence (5'-3')	PPMO target location in SARS-CoV-2 genome*
NC	CCTCTTACCTCAGTTACAATTTATA	N/A (negative control)
5'END-1	CCTGGGAAGGTATAAACCTTTAAT	1-24
5'END-2	TGTTACCTGGGAAGGTATAAACCTT	5-29
TRS-1	TTTTAAAGTTCGTTTAGAGAACAG	59-82
TRS-2	AAGTTCGTTTAGAGAACAGATCTAC	53-77
AUG-1^	AGGCTCTC**CAT**CTTACCTTTCGGT	251-275

223 *based on GenBank Accession # NC045512

224 ^ bases targeting the AUG translation start site of SARS-CoV-2 1a/b polyprotein are in boldface

225
226 **Figure legend**
227
228 **Figure 1**. Effect of PPMO on cell viability and virus growth. **A**) the effect of PPMO treatment on
229 cellular ATP level as an indicator of cell viability was carried out using uninfected cells
230 incubated for 48 hours with increasing concentrations of the indicated PPMO. ATP levels were
231 determined via luminescence readings and are shown compared to PBS-treated cells.
232 For each PPMO concentration, triplicate samples were assayed and the mean +/- standard
233 deviation is shown. **B-M**) Growth curves of SARS-CoV-2. Vero-E6 cells were treated with
234 indicated concentration of PPMO for 5 hours before infection with MOI of .01 of SARS-CoV-2.
235 Cell supernatants were collected at 12, 24, 48 and 72 hours post-infection and analyzed by
236 quantitative RT-PCR (B-G) or $TCID_{50}$/ml end-point dilution (H-M) with 3 technical repeats.
237 Cells treated with PBS only had titers similar to NC PPMO. The limit of virus detection for the

bioRxiv preprint doi: https://doi.org/10.1101/2020.09.29.319731; this version posted September 30, 2020. The copyright holder for this preprint (which was not certified by peer review) is the author/funder. All rights reserved. No reuse allowed without permission.

238 $TCID_{50}$ assay is 10^{1}/ml. This experiment was carried out twice, under similar conditions,

239 yielding similar results, and a single representative experiment is shown.

240

241

242

243

Fig 1A

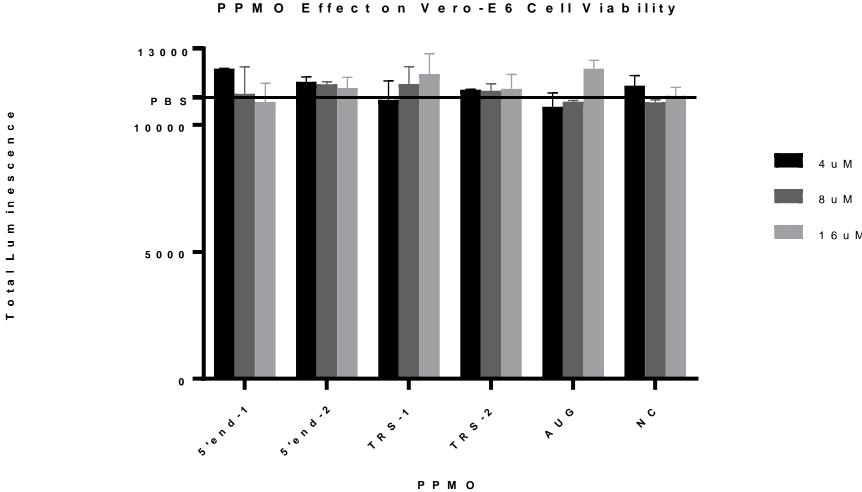

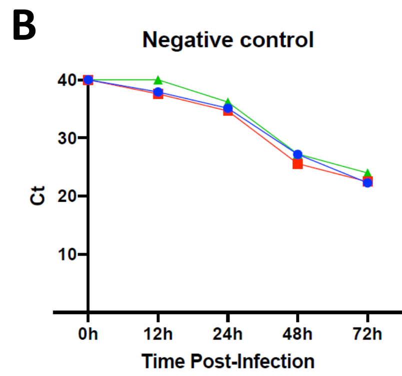
B
Negative control
Ct
0h 12h 24h 48h 72h
Time Post-Infection
16uM
8uM
4uM

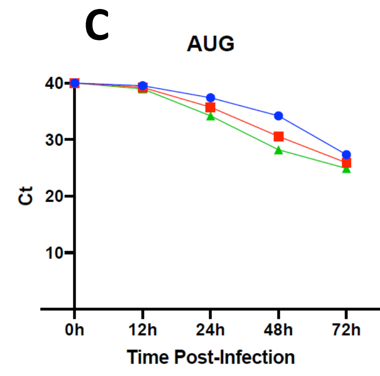
C
AUG
Ct
0h 12h 24h 48h 72h
Time Post-Infection

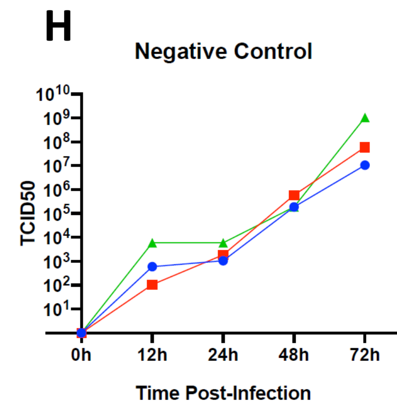
H
Negative Control
TCID50
0h 12h 24h 48h 72h
Time Post-Infection
16uM
8uM
4uM

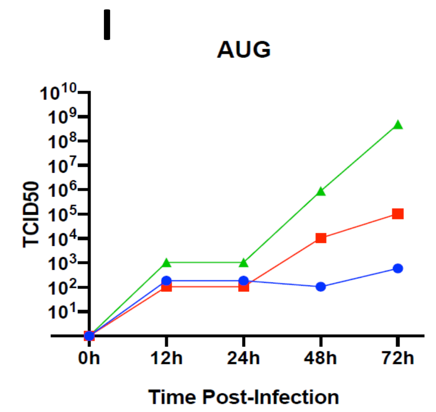
I
AUG
TCID50
0h 12h 24h 48h 72h
Time Post-Infection

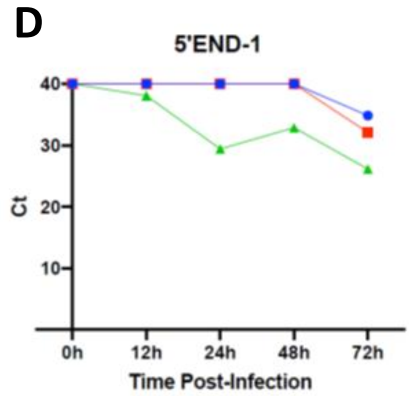
D
5'END-1
Ct
0h 12h 24h 48h 72h
Time Post-Infection
16uM
8uM
4uM

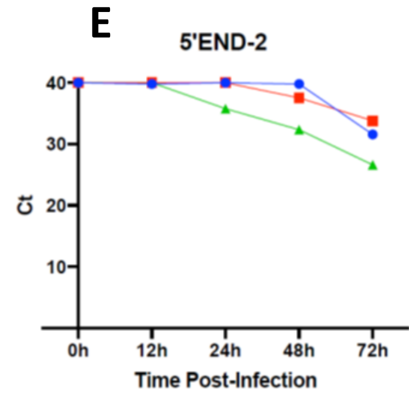
E
5'END-2
Ct
0h 12h 24h 48h 72h
Time Post-Infection

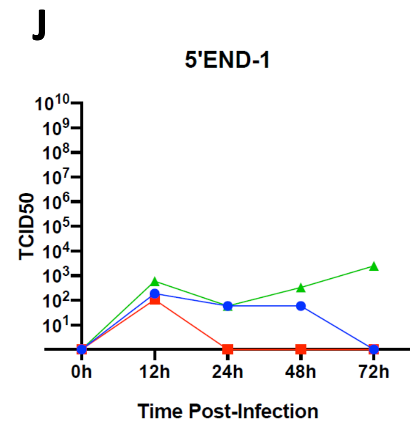
J
5'END-1
TCID50
0h 12h 24h 48h 72h
Time Post-Infection
16uM
8uM
4uM

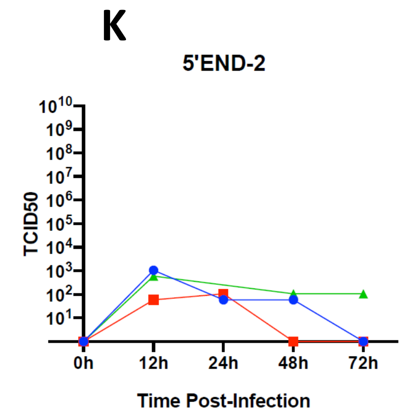
K
5'END-2
TCID50
0h 12h 24h 48h 72h
Time Post-Infection

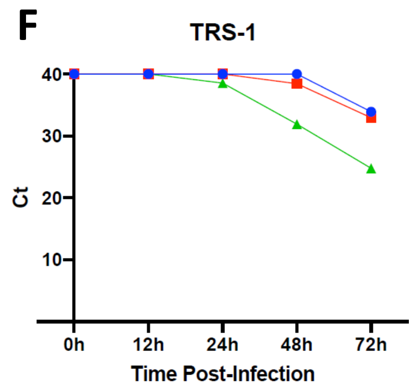
F
TRS-1
Ct
0h 12h 24h 48h 72h
Time Post-Infection
16uM
8uM
4uM

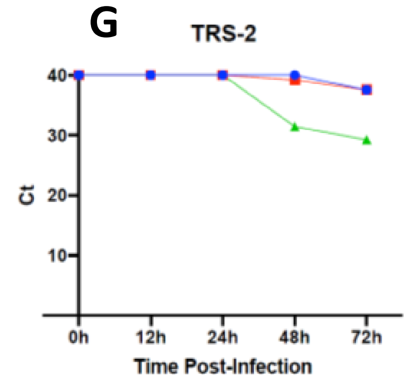
G
TRS-2
Ct
0h 12h 24h 48h 72h
Time Post-Infection

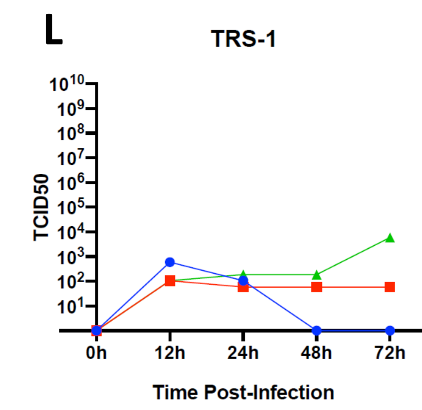
L
TRS-1
TCID50
0h 12h 24h 48h 72h
Time Post-Infection
16uM
8uM
4uM

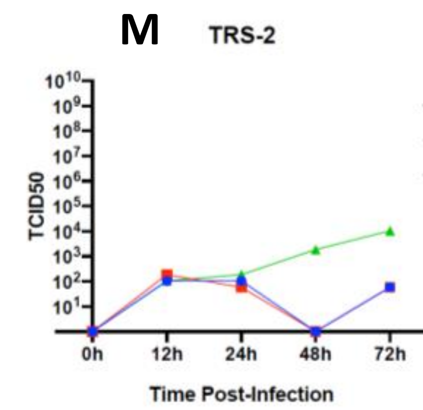
M
TRS-2
TCID50
0h 12h 24h 48h 72h
Time Post-Infection